

***In Situ* Dynamic Effusion of Trapped ZnO and CuO**

Nanoparticles in Graphene Folds

Huy Q. Ta,^{1,2,3} Alicja Bachmatiuk,^{1,4} Jamie H. Warner,⁵ Jiong Zhao,⁶ Didier Pribat,² and Mark H. Rümmeli,^{3,4,1}*

¹ Centre of Polymer and Carbon Materials, Polish Academy of Sciences, M. Curie-Skłodowskiej

34, Zabrze 41-819, Poland

² Department of Energy Science, Department of Physics, Sungkyunkwan University, Suwon 440-746, Korea

³ College of Physics, Optoelectronics and Energy & Collaborative Innovation Center of Suzhou Nano Science and Technology, Soochow University, Suzhou 215006, China.

⁴ IFW Dresden, P.O. Box D-01171 Dresden, Germany

⁵ Department of Materials, University of Oxford, Parks Road, Oxford OX1 3PH, United Kingdom

⁶ IBS Center for Integrated Nanostructure Physics, Institute for Basic Science, Sungkyunkwan University, Suwon 440-746, Korea

* Email: mhr1@suda.edu.cn

Keywords: *In situ* TEM, effusion, metal oxide nanoparticles, Graphene

Abstract In this study we examine the behavior of ZnO and CuO crystalline nanoparticles trapped within graphene folds while being irradiated with the imaging electron beam from a transmission electron microscope using an acceleration voltage of 80 kV. While trapped in the graphene folds the nanoparticles are relatively stable (as compared to particles residing on the surface of graphene), however the edges are seen to become amorphous. Eventually ruptures form at the edge of a graphene fold and the nano-crystals are observed, *in situ*, to effuse through the rupture. The transfer of mass from within a fold to the exterior is attributed to the gliding of short-lived vacancies and dislocations which occur at a rate too fast for one to observe. In the case of a ZnO nano-particle as it emerges on the outside of a fold and as the graphene erodes to form a pore the ZnO material spreads out and restructures from a wurtzite crystalline phase to that of a graphene-like phase. Later as ZnO material is sputtered away the material restructures to different wurtzite phases.

1. Introduction

Materials at the nanometer scale have properties that are remarkably different from their bulk counterparts. Metal oxide nanoparticles (NPs) which are widely used in numerous applications (*e.g.* Photo-catalysis, adsorbents, gas sensors, electrochemical, photoelectronic, *etc.*)^[1] can exhibit unique physical and chemical properties at the nanoscale due to their limited size and a high density of corner or edge surface sites. With the successful isolation of graphene in 2004 by Novoselov and Giem,^[2] metal oxide NPs decorating graphene have attracted abundant interest in the scientific community owing to their significant application in various areas such as: batteries, gas sensors and photocatalysis.^[3-6] Moreover, graphene can also enhance the properties of the host (NP) material. Hence, researchers are striving to catalog the property changes that occur with decreasing size and their behavior when decorated on graphene and more importantly, understand the reason behind novel nanomaterial properties. By learning the true nature of nanomaterials, including, metal oxide nanoparticles, scientists and engineers can design better materials for a variety of applications.

Modern high resolution transmission electron microscopes (HRTEM) offer scientists the possibility to observe and record *in situ* dynamic activity at or near the atomic level. Examples include the motion of single atoms on graphene or in carbon nanotubes,^[7, 8] migration and coalescence^[9] or atomic rearrangements^[10, 11] of metal NPs. Specimens under electron beam

irradiation can undergo several types of interaction which have been summarized by Egerton *et al.*^[12] These interactions include elastic and inelastic scattering events leading to atomic displacement or sputtering, vacancy formation, specimen heating and atomic rearrangement).

Various works show metal NPs undergoing structural rearrangement when exposed to an electron beam.^[13-16] Nano particles coated with graphitic material have also been explored. Sun *et al.*^[17] reported an *in situ* observation of metal NPs emerging out of its graphitic encapsulate through an intentionally formed hole in the graphitic coating. Due to the contraction of the graphitic shells under electron beam irradiation, internal pressure built up enabling the extrusion of metal NP material from the shell.

However, to date, no detailed study on the dynamic effusion and structural rearrangement of metal oxide particles trapped in graphene folds, driven solely by an electron beam, has been reported. In this work we present an *in situ* study on ZnO and CuO nanoparticles trapped in graphene folds using low-voltage spherical aberration-corrected transmission microscopy (LVACTEM) at 80kV.

The CuO and ZnO nanoparticles which are trapped in few-layer graphene folds are shown effuse out of defects which form at or near the crease in a graphene fold. As they emerge on the free side they spread out and restructure to a crystalline state. In the case of the ZnO nanoparticles they restructure from a bulk Wurzite form on the trapped side to a hexagonal graphene-like ZnO membrane. No additional heating is used to drive the effusion reactions.

2. Results and Discussion

The graphene membranes were initially synthesizing by chemical vapor deposition (CVD) over a Cu substrate.^[18] Thereafter the graphene material was transferred on to standard lacey carbon TEM grid. The as-produced samples were then decorated with ZnO NPs by subliming and decomposing Zinc acetylacetonate at low pressure (3×10^{-6} mbar) at 300°C. Details of the sample preparation techniques used in this work can be found elsewhere in a previous report.^[19] The CuO NPs form from remnant Cu species which occur from the etching of the copper substrate. The nanoparticles oxidize upon exposure to air. Analytical studies, confirm the structures are comprised of Zn and O as well as Cu and O. Local electron energy loss spectroscopy (EELS) was performed to determine the elements forming the particles (**Figure S1**). The EELS spectra confirmed the presence of Cu and O by the presence of the O K-edge (panel a) and Cu $L_{1,2}$ -edge (panel b)^[20] while EELS spectra for the Zn based particles show a O K-edge (panel c) and Zn $L_{1,2,3}$ -edge (panel d)^[21] confirming the presence of Zn and O.

TEM examinations of the specimen show the few-layer graphene predominantly having ZnO nanocrystals residing on the surface. The ZnO nanoparticles (ZnO NP) react with the electron beam. A typical example is provided in **Figure 1** in which a small ZnO NP starts to spread out with extended irradiation (incident current density = 5.78nA) (panel a to c). In order to confirm the presence of a ZnO structure and further characterization, multi-layer graphene was filtered out using a mask in the FFT from the original micrographs (panel d to i).^[22] This allows one to better see the ZnO nanocrystal without any interference from the graphene which leads to a Moiré pattern. The measured d-spacings were 2.80 Å (panel e) which match with the ZnO wurtzite (10 $\bar{1}$ 0) orientation.^[23] The ZnO hexagonal lattice structure is easily observed. In addition, the spreading ZnO nanocrystal seems to have some of its edges terminating at a graphene edge and appears as if the nanocrystal sits within a hole in the top (or bottom) graphene layer. The diameter

of the graphene hole increases with irradiation time expanding from ~ 3.5 nm to ~ 4.4 nm (c.f. panels d and f). This is attributed to carbon atoms at the graphene edges and graphene/ZnO interface being sputtered away due to knock on damage. This is because the knock on damage threshold for unsaturated graphene bonds (50 kV) is below the electron acceleration measurement voltage of 80 kV.^[24] As the graphene hole expands so does the ZnO crystal. However, the right side of the crystal seems open (no interface with a graphene edge is observed) and as the crystal expands the other sides maintain an interface between the graphene edges and itself suggesting an interaction or bonding occurs between the graphene edge and the ZnO nanocrystal. This is further substantiated by a significant difference to the open edge which is clearly faceted while the graphene/ZnO interface is not faceted. With extended irradiation the ZnO crystal diameter clearly shrinks and this is attributed to sputtering of the ZnO crystal. Once the amount of material at a graphene edge is very little it then tends to rearrange its crystallographic orientation, as for example seen in panel (i) in which the orientation has changed from the $(10\bar{1}0)$ orientation to the (0002) orientation.

Sometimes folds in the few-layer graphene can be observed and occasionally one finds nanoparticles encased or trapped within a fold. Examples of trapped nanocrystals in a few-layer graphene fold are provided in **Figure 2** for both a ZnO NP (panel A) and a CuO NP (panel B). The measured d spacings of 2.80 Å and 2.30 Å correspond to wurtzite ZnO $(10\bar{1}0)$ ^[23] and CuO (111) ,^[25] respectively. An image simulation of a CuO NP (111) is also provided in the inset of Figure 2.v for comparison and it shows a very good match with the experimental data. Closer examination of the TEM micrographs collected for different electron irradiation periods of up to 120 sec showed no significant change in the size or shape of both the ZnO and CuO particles. However, upon closer inspection of the particles one can see that in both cases the edges of the

NPs become amorphous, more so with longer irradiation times as highlighted by the fine yellow outlines provided in the Figure panels. The formation of the amorphous coating of the structures is attributed to knock-on damage (sputtering) of unsaturated surface atoms. The sputtered atoms then find themselves trapped in the graphene fold and so tend to form an amorphous coating around the crystalline particle. Intercalation of sputtered atoms might occur as hinted at when comparing panels vii and viii, although it is not a significant process. With extended irradiation (between 120 & 300 sec), the amorphous material at the graphene fold begins to attack the graphene fold. We first examine this process and beyond for the case of trapped ZnO as presented in **Figure 3**. Panel d shows the amorphous material at the graphene fold attacking the fold itself and in the process deforming the fold. With further irradiation a hole opens up in the graphene fold and the ZnO effuses out of the fold. We attribute the puncturing of the graphene fold to electron beam interactions at the fold/amorphous species interface, such as knock on damage. Once a small defect occurs the hole will rapidly grow since the knock damage threshold for dangling bond at the hole edge is reduced (*ca.* 50 kV).^[26] The enlarged hole at the graphene fold allows the effusing ZnO crystal to spread out laterally more easily. The driving force for the effusing material is attributed to the pressure provided by the graphene pocket (in the fold) as the graphene layers forming the pocket seek to relax back together, *viz.* compressive strain helps push material out of the pocket. This is somewhat similar to work by L. Sun *et al.*^[17] in which Au, Pt, W and Mo metals were extruded from holes in graphitic shells. Unlike our case, the holes were initially drilled using a condensed electron beam. In terms of the mass transport through the hole this is attributed to the gliding of short-lived vacancies and dislocations which occur at a rate too fast for us to observe.^[17, 27]

As the effusing ZnO nanocrystals emerge from the fold pocket they spread laterally. Closer examination of the spread out ZnO crystal structure residing outside of the fold show a d-spacing of 2.86 Å. A deeper investigation of such structures, which we conducted previously, shows these structures are graphene-like ZnO.^[19] In other words the lateral spreading of the ZnO material allow it to transform from a wurtzite phase to a 2D layered graphene-like phase, so called g-ZnO. As the irradiation and hence effusion continues, the spreading g-ZnO initially lies over a few-layer graphene support, however with extended irradiation on can see the graphene is etched by the beam (again due to knock-on damage) forming a pore (Figure 3i). A more detailed study of the g-ZnO and graphene in this region in which we filter out the graphene using Fourier transforms and masks show that the graphene under the g-ZnO has also been eroded away. **Figure S2** in the supplementary information shows this in more detail. With yet more electron beam irradiation the g-ZnO membrane erodes with open edges always being faceted as can be seen in **Figure S3**. At later stages of extended irradiation very little ZnO material is left at the edge of the graphene pore and at this stage the remaining ZnO material switches between adopting an amorphous phase or a wurtzite crystalline phase (**Figure S4**). At the same time the remaining material in the “pocket region” also erodes and changes its wurtzite crystallographic orientation (**Figure S5**) from a ZnO (10 $\bar{1}$ 0) orientation (panel a) to (0002) (panel b) to (10 $\bar{1}$ 1) (panel c) and then to (11 $\bar{2}$ 0) (panel d).^[23]

We can also observe the effusion of a different crystal structure, namely, monoclinic CuO nanoparticles trapped in a few-layer graphene folds. An example is provided in **Figure 4**. In this case no clear observation of a distortion at the fold is observed, none the less material is clearly seen to effuse from the fold and spread out. This we attribute to the rupture in the graphene being close to the fold rather than at the fold crease as illustrated in panel b of Figure 4. In this case two

ruptures appear forming two external crystals both with CuO ($\bar{1}11$)^[25] orientation (panel f). As the crystals grow they eventually touch and merge (panel g) and with extended irradiation eventually any relative rotation between the merged crystals is lost as the structure rearranges as it seeks to form a single crystal (*e.g.* panel i).^[10] Both effusion processes for the CuO and ZnO nanoparticles out of a ruptured graphene fold can also be seen in greater detail in the video provided in the supporting information.

3. Conclusion

In summary, we present *in situ* observations of the dynamic behavior of zinc oxide and copper oxide NPs driven by the (80 kV) electron beam of a TEM. Particles trapped in folds are seen to effuse out of small ruptures that form at or near a graphene crease in the fold. Pressure provided by the graphene sheets as they seek to relax back together helps drive mass out of a pocket. The effusing crystals remain crystalline. The mass transport of the crystalline nanoparticles through the rupture in a graphene fold is attributed to the gliding of short-lived vacancies and dislocations which occur at a rate too fast for us to observe.^[17, 27] Once outside a fold, the nano-crystals tend to undergo restructuring and also suffer mass loss due to sputtering.

4. Methods

1. Sample preparation

The few-layer graphene was grown over polished high purity copper foil (99.99%) using atmospheric pressure chemical vapor deposition with methane (99.999%) as the feed stock. To transfer graphene, as-produced sample was coated with PMMA (Polymethyl methacrylate). It was then floated in copper etchant (CE-100, Transene) for 30 min. After rinsing in deionized water a few times, the PMMA/graphene was then transferred on to standard lacey carbon TEM grid. After drying, the PMMA was removed by exposure to hot acetone vapor. Later the TEM grid with graphene along with Zinc acetylacetonate, $\text{Zn}(\text{acac})_2$ powder were loaded inside a glass tube (one side sealed).^[19] The glass tube was pumped down to 10^{-6} mbar by a turbo-pump and then sealed at the open end to maintain vacuum. The sealed tube and contents were then annealed at 300°C for 12 hrs.

2. Characterization

A FEI Titan³ 80-300 transmission electron microscope (TEM) with an image CEOS spherical (Cs) aberration corrector operating with an acceleration voltage of 80 kV was used. The samples were measured at room temperature. The vacuum during measurement was *ca.* 10^{-7} mbar. All image simulations used equivalent parameters to those used in the TEM experiments. The EELS (electron energy loss spectroscopy) experiments were conducted with a JEOL (ARM) 200F TEM with a probe Cs corrector operating with an acceleration voltage of 80 kV. Low-pass filtering was

applied to the micrographs to reduce noise. The filtering does not affect the final resolution of the images.

3. Image simulation

The multislice HRTEM image simulations were performed using JEMS software. For the simulations, an accelerating voltage of 80 kV and an energy spread of 0.2 eV were used. The chromatic aberration C_c was set to 1 mm, and the spherical aberration C_s was set to 1 μm . A defocus between 4 and 5 nm was used, and a defocus spread of 3 nm was implemented. These values are consistent with the experimental conditions used.

Acknowledgements

HTQ, AB and MHR thank the EOARD for support. HTQ and DP acknowledge the BK21-plus through the Ministry of Education, Korea. A.B. thanks the National Science Centre for the financial support within the frames of the Sonata Program (Grant agreement 2014/13/D/ST5/02853). M.H.R. acknowledges the DFG (DFG RU1540/15-2).

Supporting Information

Supporting Information is available from the Wiley Online Library or from the author.

Competing financial interests

The authors declare no competing financial interests.

References

- [1]. J. A. Rodríguez; M. Fernández-García, *Synthesis, Properties, and Applications of Oxide Nanomaterials*. John Wiley & Sons, Inc.: Hoboken, New Jersey, **2006**; p 379-380.
- [2]. K. S. Novoselov; A. K. Geim; S. V. Morozov; D. Jiang; Y. Zhang; S. V. Dubonos; I. V. Grigorieva; A. A. Firsov, *Science* **2004**, *306* (5696), 666.
- [3]. B. Wang; X.-L. Wu; C.-Y. Shu; Y.-G. Guo; C.-R. Wang, *J. Mater. Chem.* **2010**, *20* (47), 10661.
- [4]. K. Anand; O. Singh; M. P. Singh; J. Kaur; R. C. Singh, *Sensor. Actuat. B-Chem.* **2014**, *195*, 409.
- [5]. Z. Zhang; X. Zou; L. Xu; L. Liao; W. Liu; J. Ho; X. Xiao; C. Jiang; J. Li, *Nanoscale* **2015**, *7* (22), 10078.
- [6]. X.-Y. Zhang; H.-P. Li; X.-L. Cui; Y. Lin, *J. Mater. Chem.* **2010**, *20* (14), 2801.
- [7]. J. Zhao; Q. Deng; S. M. Avdoshenko; L. Fu; J. Eckert; M. H. Rummeli, *Proc. Natl. Acad. Sci. U.S.A.* **2014**, *111* (44), 15641.
- [8]. J. H. Warner; Y. Ito; M. H. Rummeli; T. Gemming; B. Büchner; H. Shinohara; G. A. D. Briggs, *Phys. Rev. Lett.* **2009**, *102* (19), 195504.
- [9]. J. Li; Z. Wang; C. Chen; S. Huang, *Sci. Rep.* **2014**, *4*, 5521.
- [10]. J. H. Warner; M. H. Rummeli; A. Bachmatiuk; M. Wilson; B. Büchner, *ACS Nano* **2010**, *4* (1), 470.
- [11]. J. H. Warner; S. R. Plant; N. P. Young; K. Porfyrakis; A. I. Kirkland; G. A. D. Briggs, *ACS Nano* **2011**, *5* (2), 1410.
- [12]. R. F. Egerton; P. Li; M. Malac, *Micron* **2004**, *35* (6), 399.
- [13]. M. O. Cichocka; J. Zhao; A. Bachmatiuk; H. T. Quang; S. M. Gorantla; I. G. Gonzalez-Martinez; L. Fu; J. Eckert; J. H. Warner; M. H. Rummeli, *RSC Adv.* **2014**, *4* (90), 49442.
- [14]. L. C. Gontard; R. E. Dunin-Borkowski, *Micron* **2015**, *70*, 41.
- [15]. M. Tanaka; M. Takeguchi; K. Furuya, *Micron* **2002**, *33* (5), 441.
- [16]. D. J. Smith; A. K. Petford-Long; L. R. Wallenberg; J. O. Bovin, *Science* **1986**, *233*, 872.
- [17]. L. Sun; A. V. Krashennnikov; T. Ahlgren; K. Nordlund; F. Banhart, *Phys. Rev. Lett.* **2008**, *101* (15), 156101.
- [18]. G. H. Han; F. Güneş; J. J. Bae; E. S. Kim; S. J. Chae; H. J. Shin; J. Y. Choi; D. Pribat; Y. H. Lee, *Nano Lett.* **2011**, *11* (10), 4144.
- [19]. H. Q. Ta; A. Bachmatiuk; A. Dianat; F. Ortmann; J. Zhao; J. H. Warner; J. Eckert; G. Cuniberti; M. H. Rummeli, *ACS Nano* **2015**, *9* (11), 11408.
- [20]. F. Hofer; P. Golob, *Ultramicroscopy* **1987**, *21* (4), 379.
- [21]. Y. Ding; Z. L. Wang, *J. Electron Microsc.* **2005**, *54* (3), 287.
- [22]. J. H. Warner; M. H. Rummeli; T. Gemming; B. Büchner; G. A. D. Briggs, *Nano Lett.* **2009**, *9* (1), 102.
- [23]. M. Y. Ge; H. P. Wu; L. Niu; J. F. Liu; S. Y. Chen; P. Y. Shen; Y. W. Zeng; Y. W. Wang; G. Q. Zhang; J. Z. Jiang, *J. Crys. Growth* **2007**, *305* (1), 162.
- [24]. J. Kotakoski; D. Santos-Cottin; A. V. Krashennnikov, *ACS Nano* **2012**, *6* (1), 671.
- [25]. S. L. Cheng; M. F. Chen, *Nanoscale Res. Lett.* **2012**, *7* (1), 119.
- [26]. J. H. Warner; M. H. Rummeli; L. Ge; T. Gemming; B. Montanari; N. M. Harrison; B. Büchner; G. A. D. Briggs, *Nat. Nanotechnol.* **2009**, *4* (8), 500.
- [27]. J. C. M. Li, *Trans. Metall. Soc. AIME* **1963**, *227*, 239.

Figures

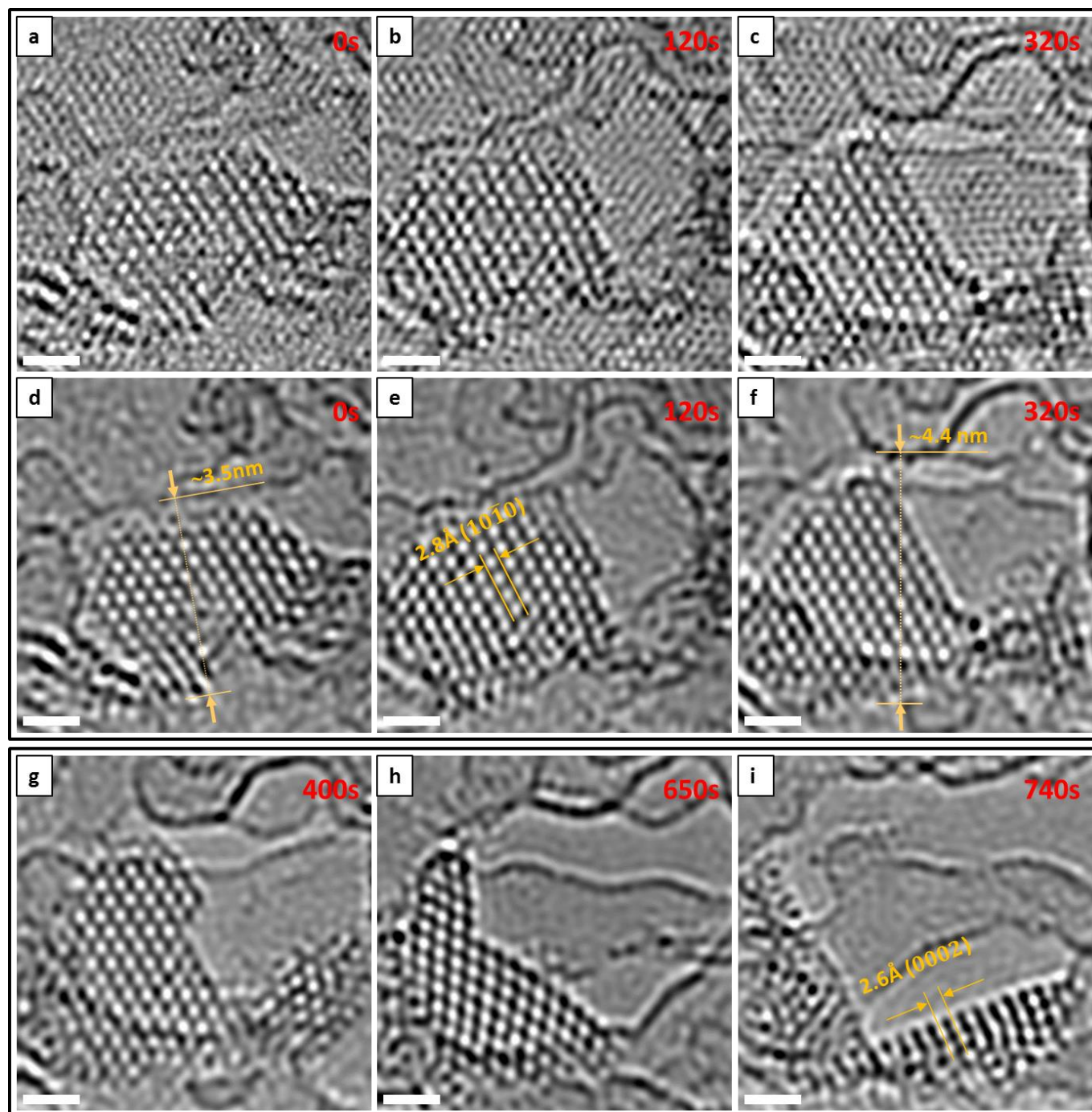


Figure 1.

HRTEM images showing the dynamic behavior of ZnO nano-crystals while under electron beam irradiation (a-c) a ZnO nanocrystal over few-layer graphene with Moiré pattern is spreading out under electron beam irradiation, (d-f) the hexagonal lattice structure of ZnO ($10\bar{1}0$) was shown after filtering graphene underneath, graphene hole also getting larger. (g-i) Graphene and ZnO keep sputtering out, ZnO crystal is collapsed with extended irradiation. All scale bars = 1 nm.

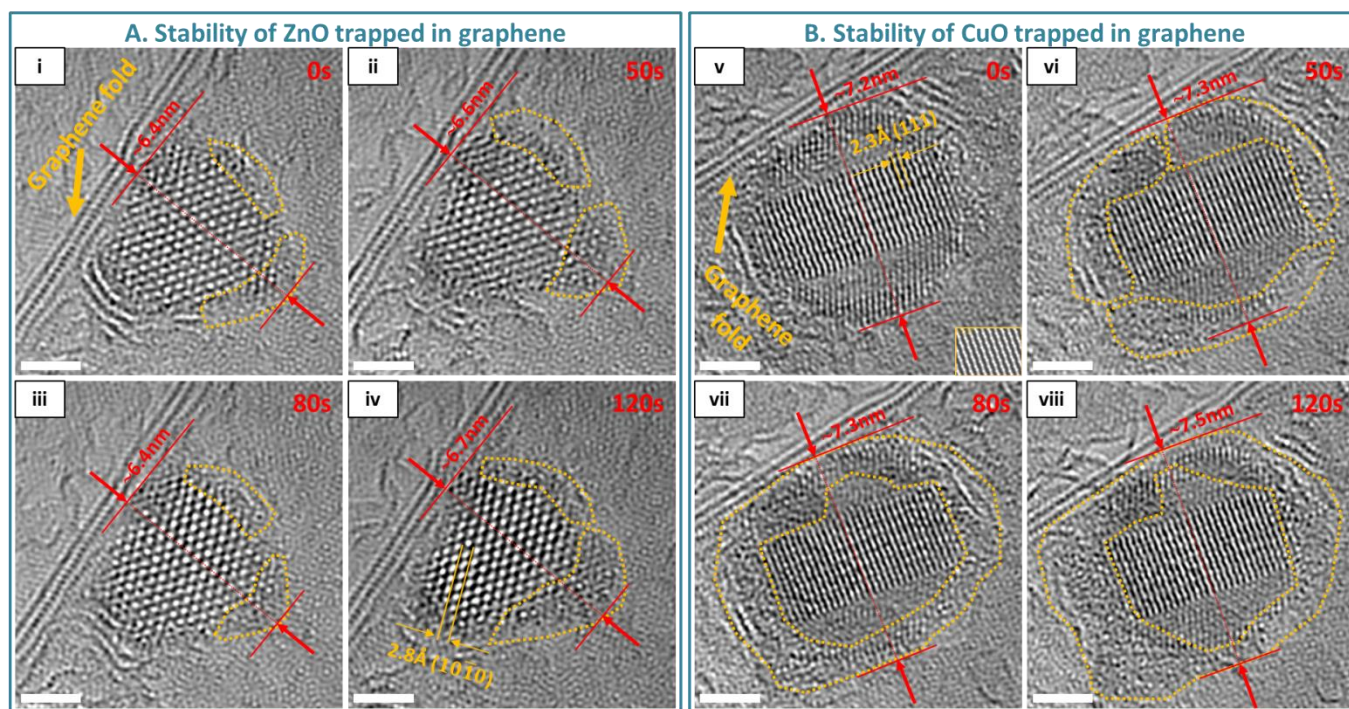


Figure 2.

Behavior of ZnO and CuO NPs encapsulated in graphene fold. (A) Stability of trapped ZnO NP under electron beam irradiation, particle size varies in the range of 6.4 to 6.7(nm) with stable shape in 120sec irradiation. Amorphous forming mostly in the right side of the particles. (B) Stability of trapped CuO NP under electron beam irradiation, particle size varies in the range of 7.2 to 7.5(nm), Thick amorphous forming around the edge of the particle. Inset Figure v shows image simulation of CuO NP. All scale bars = 2nm.

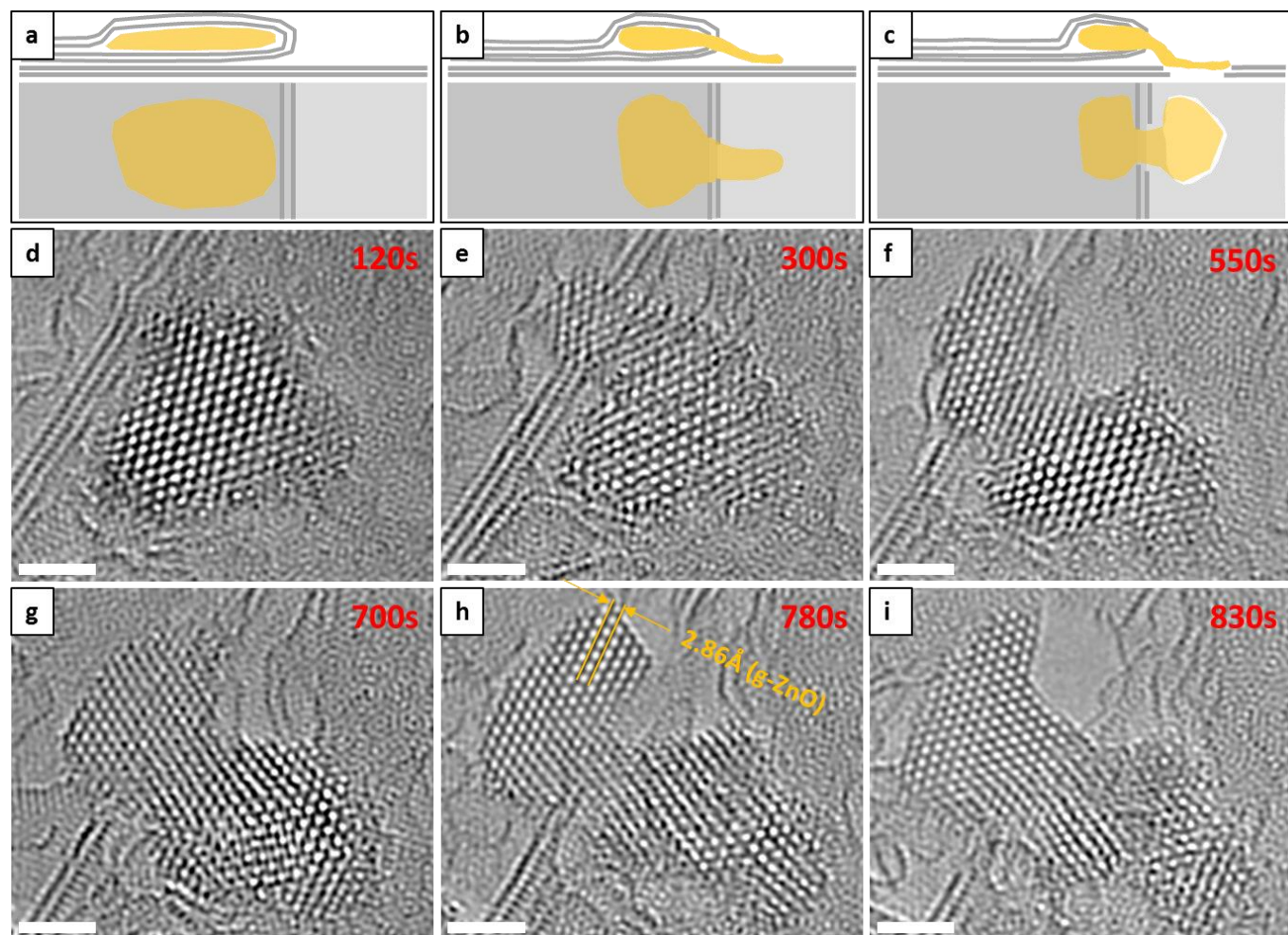


Figure 3.

The effusion process of ZnO NP based on contraction of graphene fold under electron beam irradiation and forming g-ZnO freestanding membrane. (a-c) schematic of effusion through folding graphene. (d-g) TEM images of effusion process. (h-i) TEM image of formation of g-ZnO freestanding membrane in graphene hole. All scale bars = 2nm.

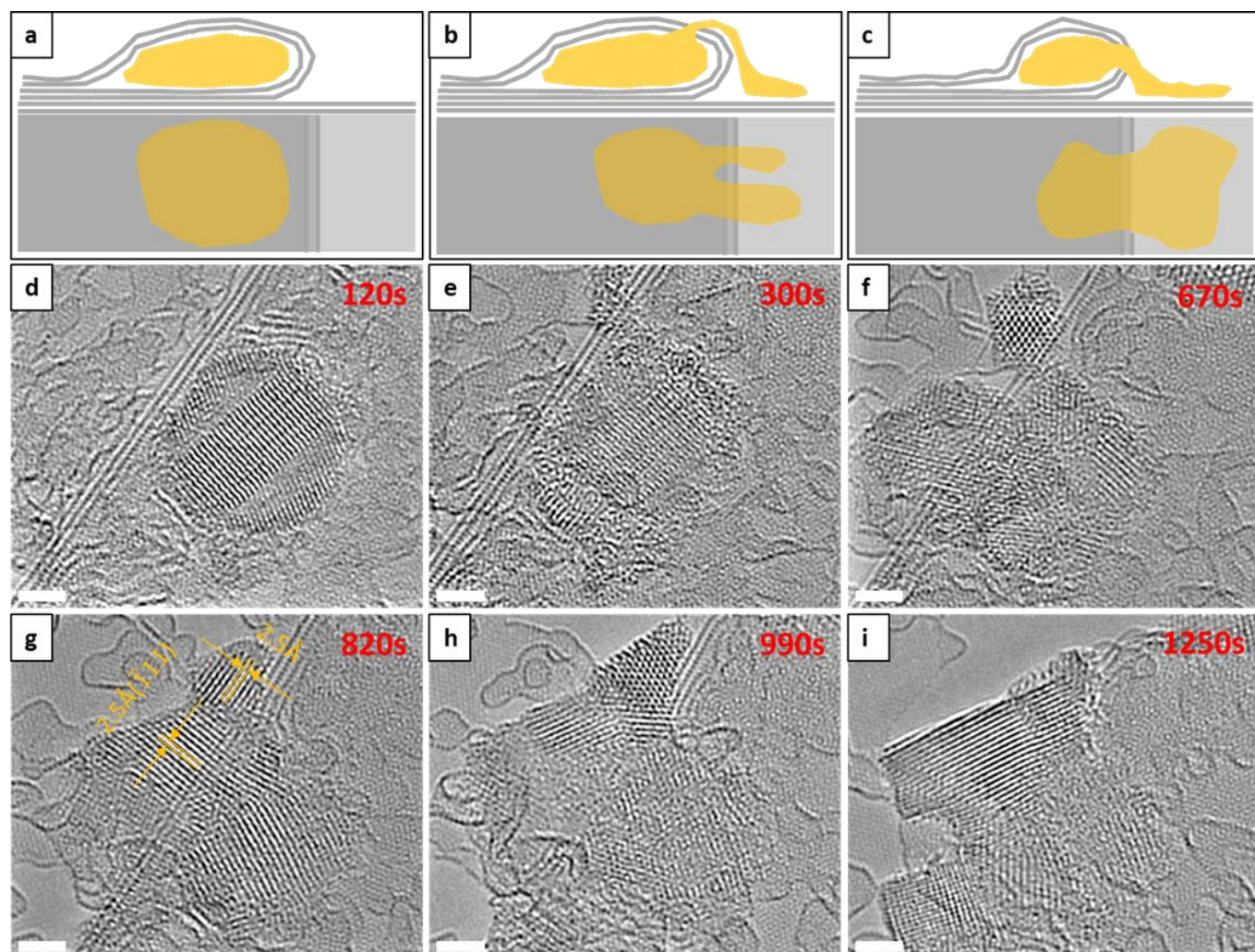


Figure 4.

The effusion process of CuO NP based on contraction of graphene fold under electron beam irradiation and coalescence between two NPs process. (a-c) schematic of effusion through graphene. (d-g) TEM images of effusion process. (h-i) TEM images of Coalescence between two CuO($\bar{1}11$) NPs. All scale bars = 2nm.

Supplementary Information

***In Situ* Dynamic Effusion of Trapped ZnO and CuO
Nanoparticles in Graphene Folds**

Huy Q. Ta,^{1,2,3} Alicja Bachmatiuk,^{1,4} Jamie H. Warner,⁵ Jiong Zhao,⁶ Didier Pribat,² and Mark H. Rümmeli,^{3,4,1}*

¹ Centre of Polymer and Carbon Materials, Polish Academy of Sciences, M. Curie-Skłodowskiej 34, Zabrze 41-819, Poland

² Department of Energy Science, Department of Physics, Sungkyunkwan University, Suwon 440-746, Korea

³ College of Physics, Optoelectronics and Energy & Collaborative Innovation Center of Suzhou Nano Science and Technology, Soochow University, Suzhou 215006, China.

⁴ IFW Dresden, P.O. Box D-01171 Dresden, Germany

⁵ Department of Materials, University of Oxford, Parks Road, Oxford OX1 3PH, United Kingdom

⁶ IBS Center for Integrated Nanostructure Physics, Institute for Basic Science, Sungkyunkwan University, Suwon 440-746, Korea

* Email: mhr1@suda.edu.cn

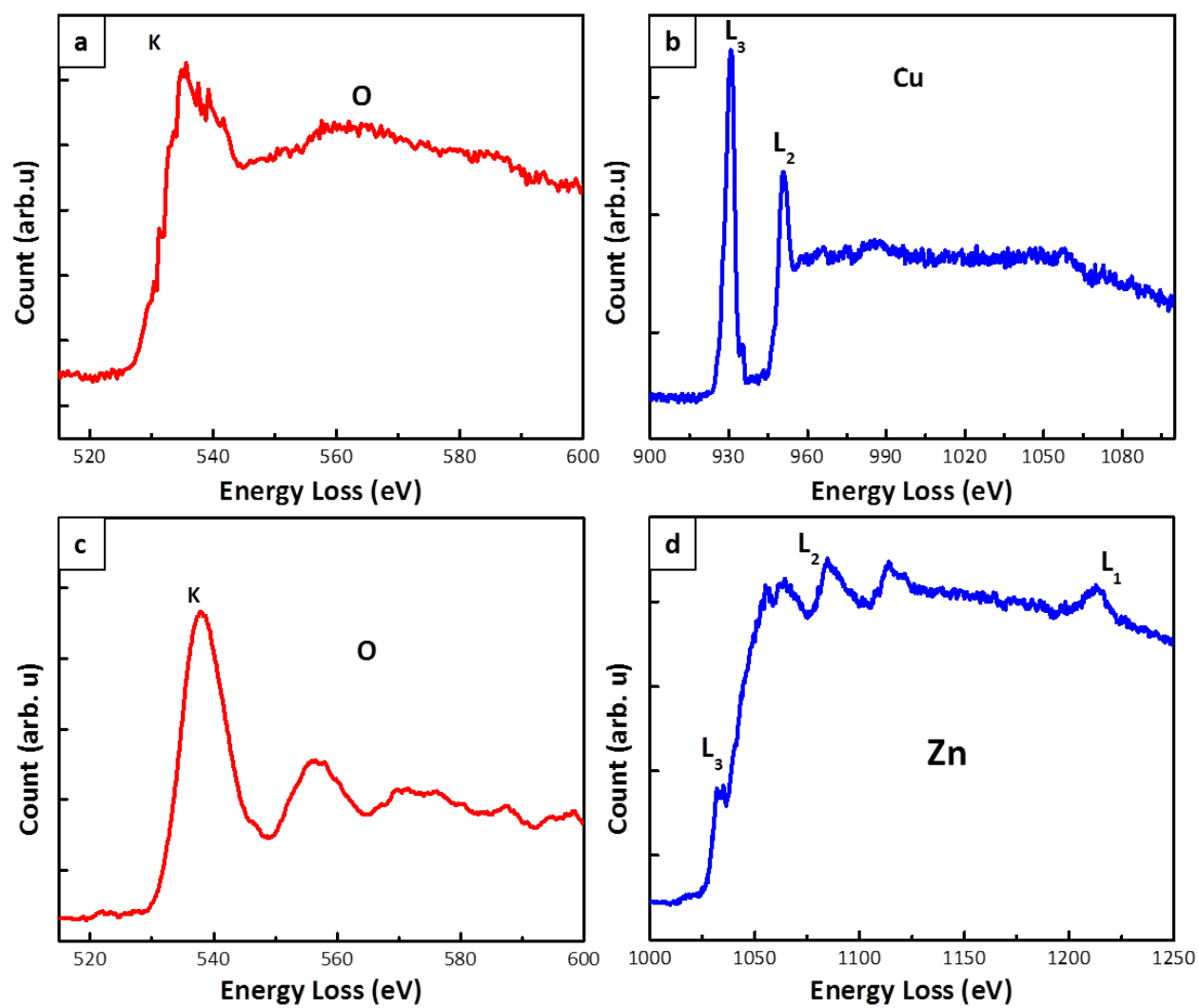


Figure S1.

EELS spectra confirmation presence Cu, O in CuO NP and Zn, O in ZnO NP. (a, b) Oxygen K-edge and Cu L_{1,2}-edge EELS spectra of CuO NP. (c-d) Oxygen K-edge and Zinc L_{1,2,3}-edge EELS spectra of ZnO.

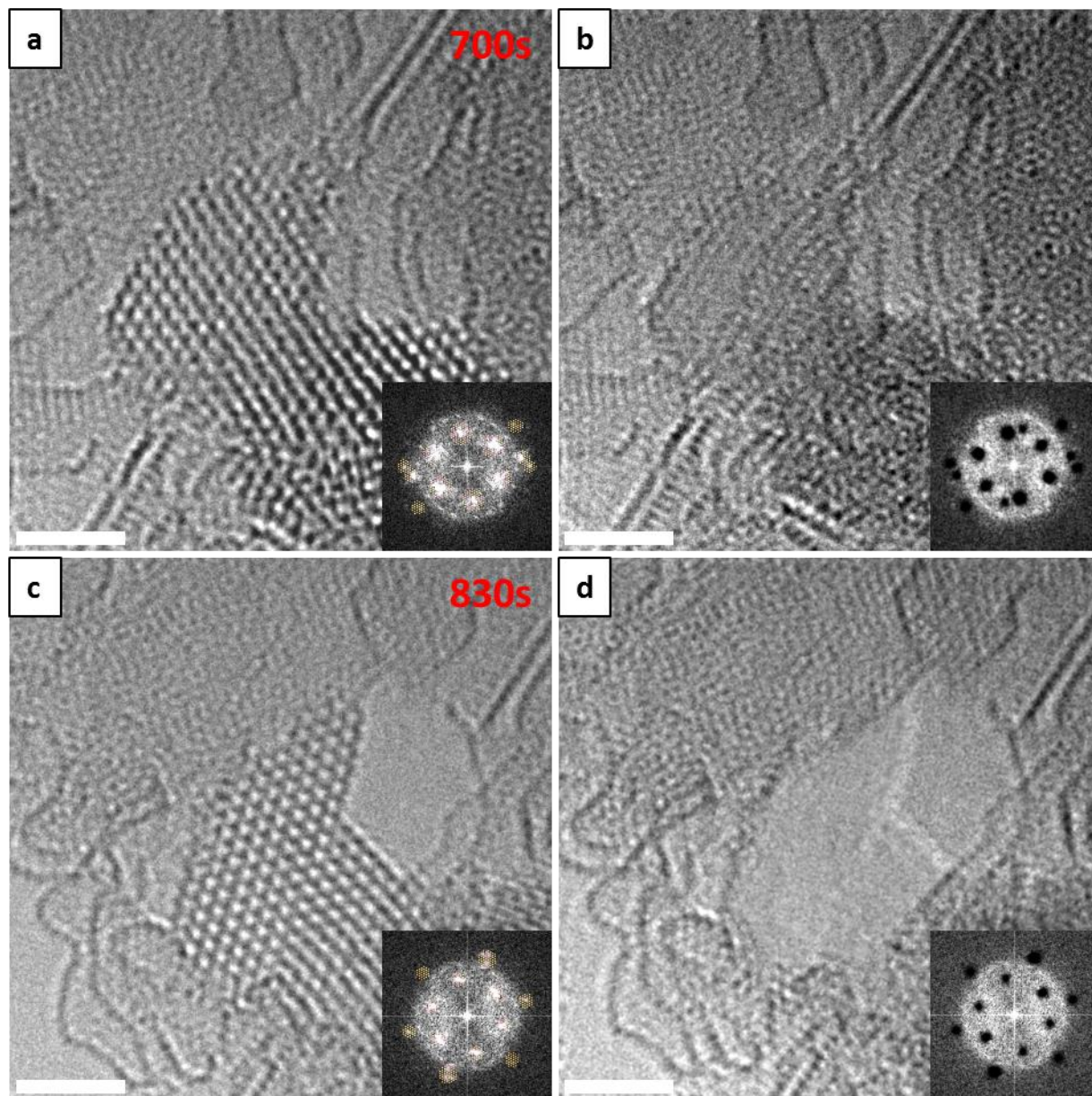


Figure S2. Comparison of free-standing g-ZnO suspended membrane in graphene hole to ZnO NP reside on graphene. (a) An original TEM image of ZnO NP. Inset Figure shows Fast Fourier transform of the ZnO NP and graphene in (a), with mask spots. (b) Inverse-FFT image which filtered out the ZnO reflex exposing graphene beneath. (c) An original TEM image of g-ZnO membrane. Inset Figure shows Fast Fourier transform of the g-ZnO membrane and graphene in (c), with mask spots. (d) Inverse-FFT image which has the g-ZnO reflex filtered out exposing vacuum beneath the membrane (i.e. no graphene). All scale bars = 2nm.

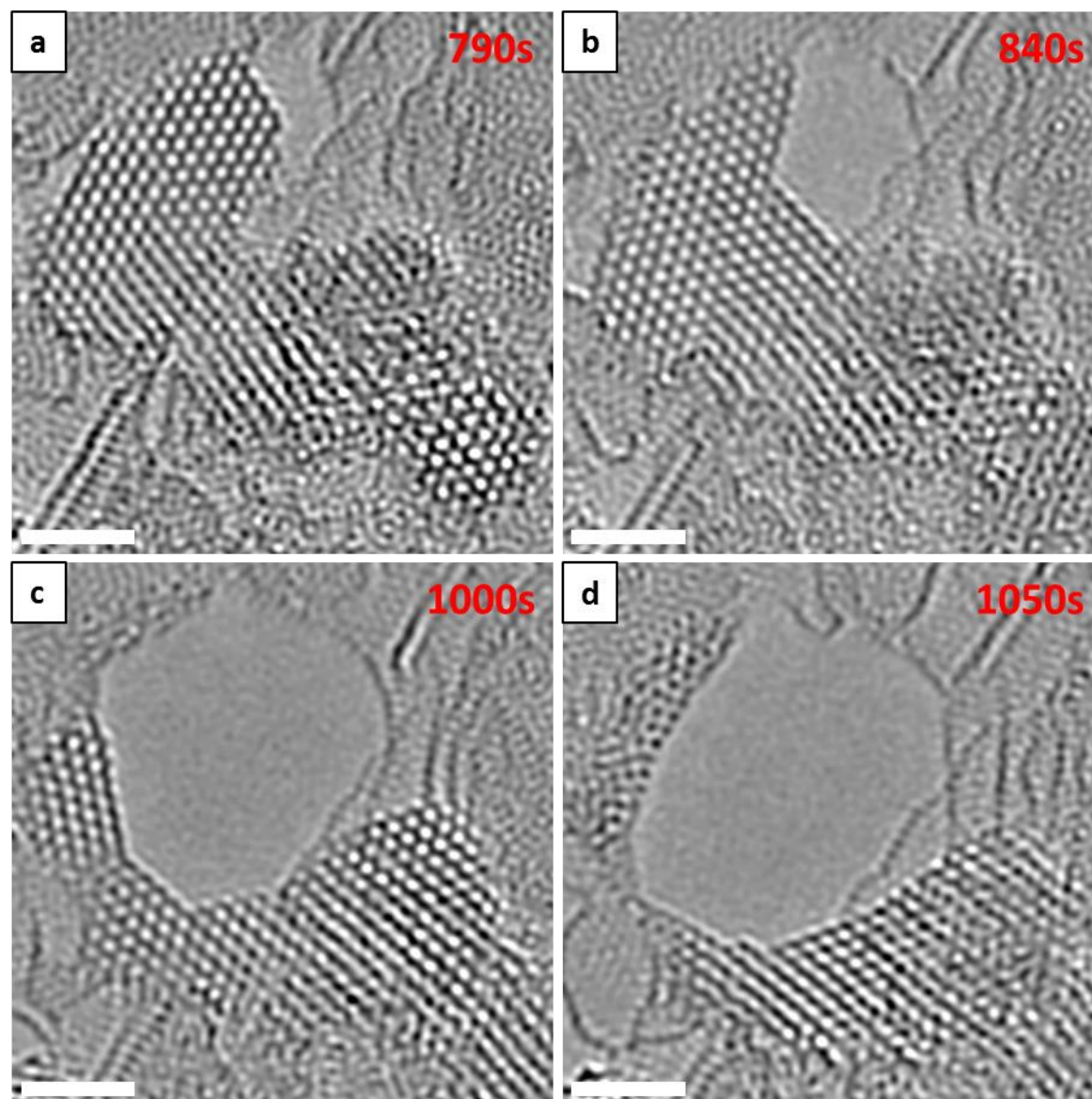


Figure S3. Behavior of freestanding g-ZnO after extended electron beam irradiation. (a-c) TEM images of process of atoms were sputtered away with faceting in the back. (d) Membrane collapsed, Zn and O atoms attached along the graphene. All scale bars =2 nm.

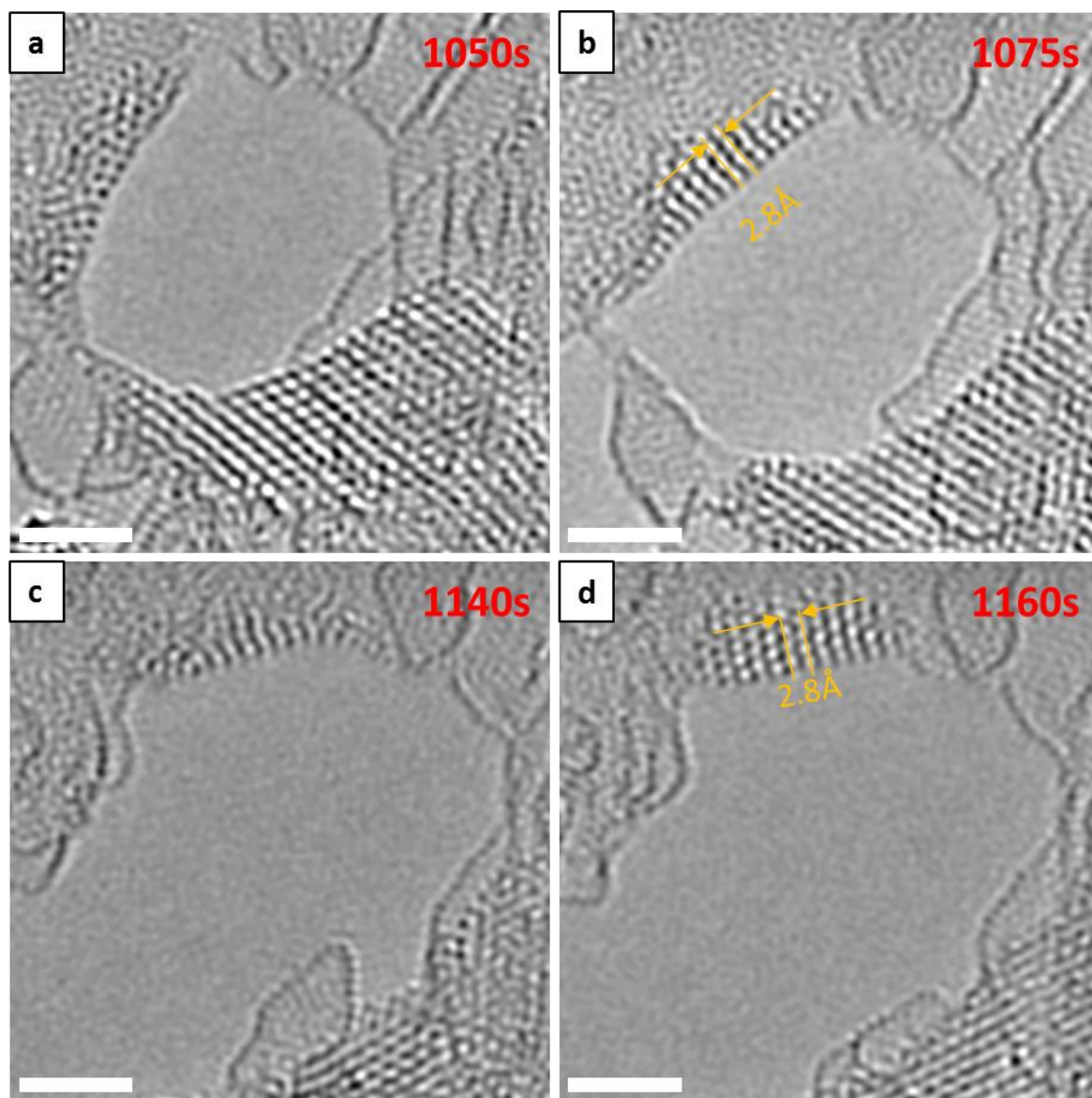


Figure S4. Small cluster of ZnO switching back and forward from an ordered crystalline structure to an amorphous structure under electron beam irradiation. All scale bars = 2nm.

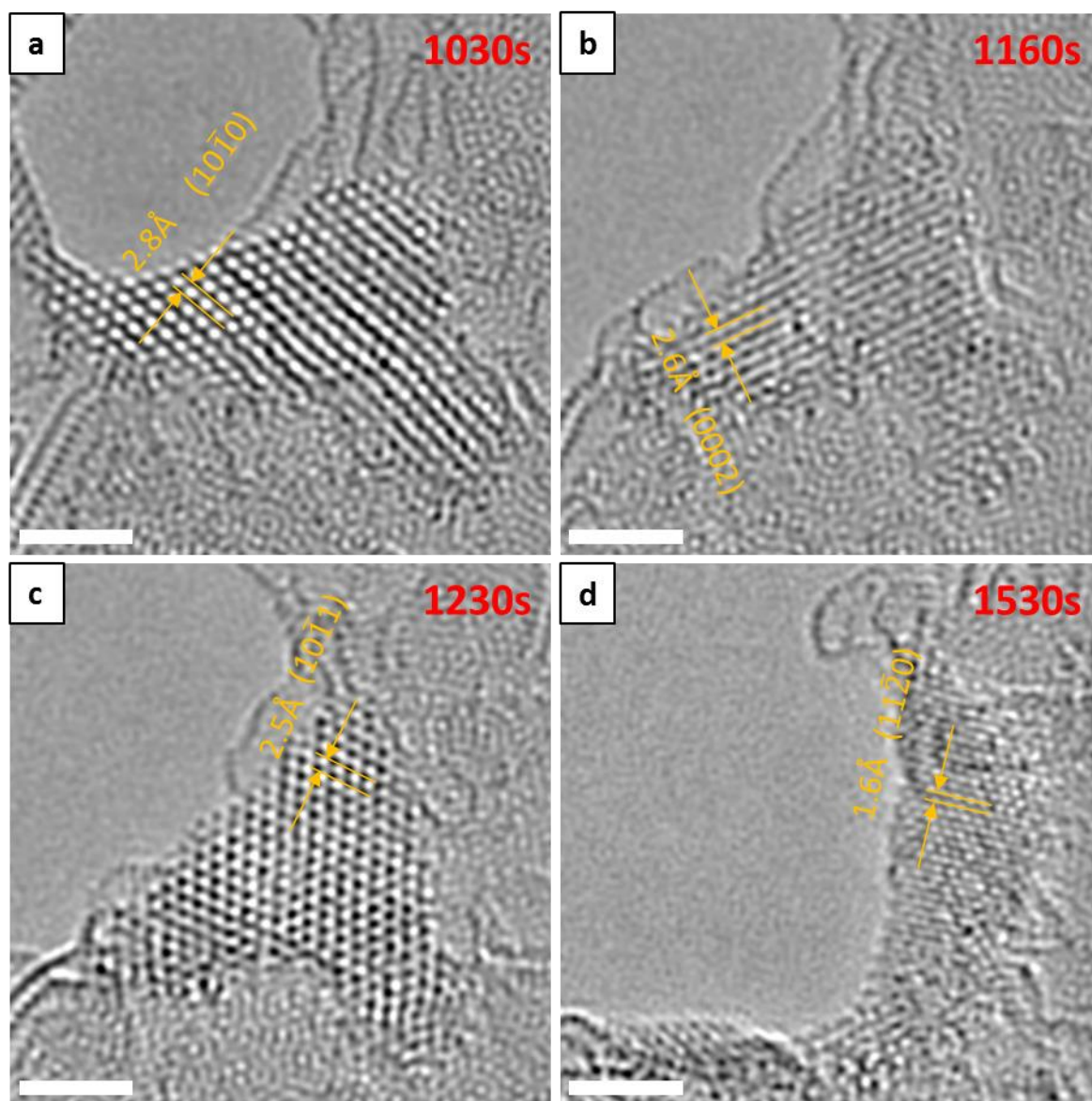


Figure S5. Reconstruction of ZnO crystal structure under electron beam. (a) ZnO($10\bar{1}0$). (b) ZnO(0002). (c) ZnO($10\bar{1}1$). (d) ZnO($11\bar{2}0$). All scale bars= 2nm

Graphical Abstract

